

Learning Locality-Constrained Collaborative Representation for Robust Face Recognition

Xi PENG^a, Lei ZHANG^{a,*}, ZHANG Yi^a, Kok Kiong Tan^b

^aMachine Intelligence Laboratory, College of Computer Science, Sichuan University, Chengdu, 610065, China.

^bDepartment of Electrical and Computer Engineering, National University of Singapore, Engineering Drive 3, Singapore 117576.

Abstract

The model of low-dimensional manifold and sparse representation are two well-known concise models that suggest each data can be described by a few characteristics. Manifold learning is usually investigated for dimension reduction by preserving some expected local geometric structures from the original space to a low-dimensional one. The structures are generally determined by using pairwise distance, e.g., Euclidean distance. Alternatively, sparse representation denotes a data point as a linear combination of the points from the same subspace. In practical applications, however, the nearby points in terms of pairwise distance may not belong to the same subspace, and vice versa. Consequently, it is interesting and important to explore how to get a better representation by integrating these two models together. To this end, this paper proposes a novel coding algorithm, called Locality-Constrained Collaborative Representation (LCCR), which improves the robustness and discrimination of data representation by introducing a kind of local consistency. The locality term derives from a biologic observation that the similar inputs have similar code. The objective function of LCCR has an analytical solution, and it does not involve local minima. The empirical studies based on four public facial databases, ORL, AR, Extended Yale B, and Multiple PIE, show that LCCR is promising in recognizing human faces from frontal views with varying expression and illumination, as well as various corruptions and occlusions.

Keywords: Non-sparse representation, sparse representation, locality consistency, ℓ^2 -minimization, partial occlusions, additive noise, non-additive noise, robustness.

1. Introduction

Sparse representation has become a powerful method to address problems in pattern recognition and computer vision, which assumes that each data point $\mathbf{x} \in \mathbb{R}^m$ can be encoded as a linear combination of other points. In mathematically, $\mathbf{x} = \mathbf{D}\mathbf{a}$, where \mathbf{D} is a dictionary whose columns consist of some data points, and \mathbf{a} is the representation of \mathbf{x} over \mathbf{D} . If most entries of \mathbf{a} are zeros, then \mathbf{a} is called a sparse representation. Generally, it can be achieved by solving

$$(P_0) : \quad \min \|\mathbf{a}\|_0 \quad \text{s.t.} \quad \mathbf{x} = \mathbf{D}\mathbf{a},$$

where $\|\cdot\|_0$ denotes ℓ^0 -norm by counting the number of nonzero entries in a vector. P_0 is difficult to solve since it is a NP-hard problem. Recently, compressive sensing theory [1, 2] have found that the solution of P_0 is equivalent to that of ℓ^1 -minimization problem ($P_{1,1}$) when \mathbf{a} is highly sparse.

$$(P_{1,1}) : \quad \min \|\mathbf{a}\|_1 \quad \text{s.t.} \quad \mathbf{x} = \mathbf{D}\mathbf{a},$$

where ℓ^1 -norm $\|\cdot\|_1$ sums the absolute value of all entries in a vector. $P_{1,1}$ is convex and can be solved by a large amount of convex optimization methods, such as basis pursuit (BP) [3], least angle regression (LARS) [4]. In [5], Yang et al. make a comprehensive survey for some popular optimizers.

*Corresponding author

Email addresses: pangsaai@gmail.com (Xi PENG), leizhang@scu.edu.cn (Lei ZHANG), zhangyi@scu.edu.cn (ZHANG Yi), kktan@nus.edu.sg (Kok Kiong Tan)

15 Benefiting from the emergence of compressed sensing theory, sparse coding has been widely used for various
16 tasks, e.g., subspace learning [6], spectral clustering [7, 8] and matrix factorization [9]. In these works, Wright et
17 al. [10] reported a remarkable method that passes sparse representation through a nearest feature subspace classifier,
18 named sparse representation based classification (SRC). SRC has achieved attractive performance in robust face recog-
19 nition and has motivated a large amount of works such as [11, 12, 13]. The work implies that sparse representation
20 plays an important role in face recognition under the framework of nearest subspace classification [14].

21 However, is ℓ^1 -norm based sparsity really necessary to improve the performance of face recognition? Several
22 recent works directly or indirectly examined this problem. Yang et al. [15] discussed the connections and differences
23 between ℓ^1 -optimizer and ℓ^0 -optimizer for SRC. They show that the success of SRC should attribute to the mech-
24 anism of ℓ^1 -optimizer which selects the set of support training samples for the given testing sample by minimizing
25 reconstruction error. Consequently, Yang et al. pointed out that the global similarity derived from ℓ^1 -optimizer but
26 sparsity derived from ℓ^0 -optimizer is more critical for pattern recognition. Rigamonti et al. [16] compared the dis-
27 crimination of two different data models. One is the ℓ^1 -norm based sparse representation, and the other model is
28 produced by passing input into a simple convolution filter. Their result showed that two models achieve a similar
29 recognition rate. Therefore, ℓ^1 -norm based sparsity is actually not as essential as it seems in the previous claims. Shi
30 et al. [17] provided a more intuitive approach to investigate this problem by removing the ℓ^1 -regularization term from
31 the objective function of SRC. Their experimental results showed that their method achieves a higher recognition rate
32 than SRC if the original data is available. Zhang et al. [18] replaced the ℓ^1 -norm by the ℓ^2 -norm, and their experimen-
33 tal results again support the views that ℓ^1 -norm based sparsity is not necessary to improve the discrimination of data
34 representation. Moreover, we have noted that Naseem et al. [19] proposed Linear Regression Classifier (LRC) which
35 has the same objective function with Shi’s work. The difference is that Shi et al. aimed to explore the role of sparsity
36 while Naseem et al. focused on developing an effective classifier for face recognition.

37 As another extensively-studied concise model, manifold learning is usually investigated for dimension reduction
38 by learning and embedding local consistency of original data into a low-dimensional representation [20, 21, 22]. Local
39 consistency means that nearby data points share the same properties, which is hardly reflected in linear representation.

40 Recently, some researchers have explored the possibility of integrating the locality (local consistency) with the
41 sparsity together to produce a better data model. Baraniuk et al. [23] successfully bridged the connections between
42 sparse coding and manifold learning, and have founded the theory for random projections of smooth manifold; Ma-
43 jumdar et al. [24] investigated the effectiveness and robustness of random projection method in classification task.
44 Moreover, Wang et al. [25] proposed a hierarchical images classification method named locality-constrained linear cod-
45 ing (LLC) by introducing dictionary learning into Locally Linear Embedding (LLE) [26]. Chao et al. [27] presented
46 an approach to unify group sparsity and data locality by introducing the term of ridge regression into LLC; Yang et
47 al. [28] incorporated the prior knowledge into the coding process by iteratively learning a weight matrix of which the
48 atoms measure the similarity between two data points.

49 In this paper, we proposed and formulated a new kind of local consistency into the linear coding paradigm by en-
50 forcing **the similar inputs (neighbors) produce similar codes**. The idea is motivated by an observation in biological
51 finds [29] which shows that L2/3 of rat visual cortex activates the same collection of neurons in response to leftward
52 and rightward drifting gratings. Figure 1 show an example to illustrate the motivation. There are three face images
53 A , B and C selected from two different individuals, where A and B came from the same person. This means that A
54 and B lie on the same subspace and could represent with each other. Figure 1(b) is a real example corresponding to
55 Figure 1(a). Either from the Eigenface matrices or the coefficients of the two coding schemes, we can see that the
56 similarity between A and B is much higher than the similarity between C and either of them.

57 Based on the observation, we proposed a representation learning method for robust face recognition, named as
58 Locality-Constrained Collaborative Representation (LCCR), which not aims to obtain a representation that could
59 reconstruct the input with the minimal residual but simultaneously reconstruct the input and its neighborhood such that
60 the codes are as similar as possible. Furthermore, the objective function of LCCR has an analytic solution, does not
61 involve local minima. Extensive experiments show that LCCR outperforms SRC [10], LRC [17, 19], CRC-RLS [18],
62 CESR [13], LPP [30], and linear SVM in the context of robust face recognition.

63 Except in some specified cases, lower-case bold letters represent column vectors and upper-case bold ones repre-
64 sent matrices, \mathbf{A}^T denotes the transpose of the matrix \mathbf{A} , \mathbf{A}^{-1} represents the pseudo-inverse of \mathbf{A} , and \mathbf{I} is reserved for
65 identity matrix.

66 The remainder of paper is organized as follows: Section 2 introduces three related approaches for face recogni-

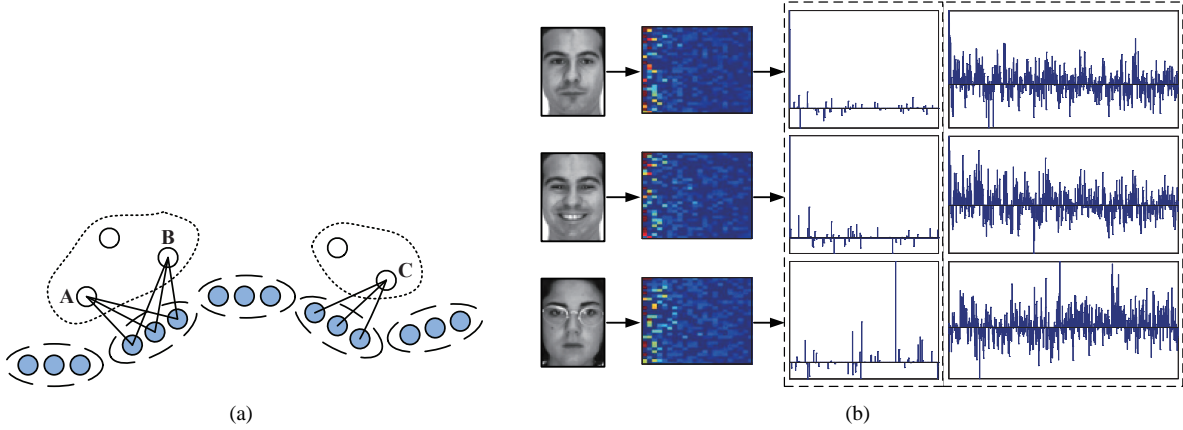


Figure 1: A key observation. (a) Three face images from two different sub-manifolds are linked to their corresponding neighbors, respectively. (b) The first column includes three images which correspond to the points A , B and C in Figure 1(a); The second column shows the Eigenface feature matrices for the testing images; The third column includes two parts: the left part is the coefficients of SRC [10], and the right one is of CRC-RLS [18]. From the results, we could see that the representations of nearby points are more similar than that of non-neighboring points, i.e., local consistency could be defined as the similar inputs have similar codes.

tion based on data representation, i.e., SRC [10], LRC [17, 19] and CRC-RLS [18]. Section 3 presents our LCCR algorithm. Section 4 reports the experiments on several facial databases. Finally, Section 5 contains the conclusion.

2. Preliminaries

We consider a set of N facial images collected from L subjects. Each training image, which is denoted as a vector $\mathbf{d}_i \in \mathbb{R}^M$, corresponds to the i th column of a dictionary $\mathbf{D} \in \mathbb{R}^{M \times N}$. Without generality, we assume that the columns of \mathbf{D} are sorted according to their labels.

2.1. Sparse representation based classification

Sparse coding aims at finding the most sparse solution of $P_{1,1}$. However, in many practical problems, the constraint $\mathbf{x} = \mathbf{D}\mathbf{a}$ cannot hold exactly since the input \mathbf{x} may include noise. Wright et al. [10] relaxed the constraint to $\|\mathbf{x} - \mathbf{D}\mathbf{a}\|_2 \leq \varepsilon$, where $\varepsilon > 0$ is the error tolerance, then, $P_{1,1}$ is rewritten as:

$$(P_{1,2}) : \quad \min \|\mathbf{a}\|_1 \quad \text{s.t.} \quad \|\mathbf{x} - \mathbf{D}\mathbf{a}\|_2 \leq \varepsilon.$$

Using Lagrangian method, $P_{1,2}$ can be transformed to the following unconstrained optimization problem:

$$(P_{1,3}) : \quad \underset{\mathbf{a}}{\operatorname{argmin}} \|\mathbf{x} - \mathbf{D}\mathbf{a}\|_2^2 + \lambda \|\mathbf{a}\|_1,$$

where the scalar $\lambda \geq 0$ balances the importance between the reconstruction error of \mathbf{x} and the sparsity of code \mathbf{a} . Given a testing sample $\mathbf{x} \in \mathbb{R}^M$, its sparse representation $\mathbf{a}^* \in \mathbb{R}^N$ can be computed by solving $P_{1,2}$ or $P_{1,3}$.

After getting the sparse representation of \mathbf{x} , one infers its label by assigning \mathbf{x} to the class that has the minimum residual:

$$r_i(\mathbf{x}) = \|\mathbf{x} - \mathbf{D} \cdot \delta_i(\mathbf{a}^*)\|_2, \quad (1)$$

$$\operatorname{identity}(\mathbf{x}) = \underset{i}{\operatorname{argmin}} \{r_i(\mathbf{x})\}. \quad (2)$$

where the nonzero entries of $\delta_i(\mathbf{a}^*) \in \mathbb{R}^N$ are the entries in \mathbf{a}^* that are associated with i th class, and $\operatorname{identity}(\mathbf{x})$ denotes the label for \mathbf{x} .

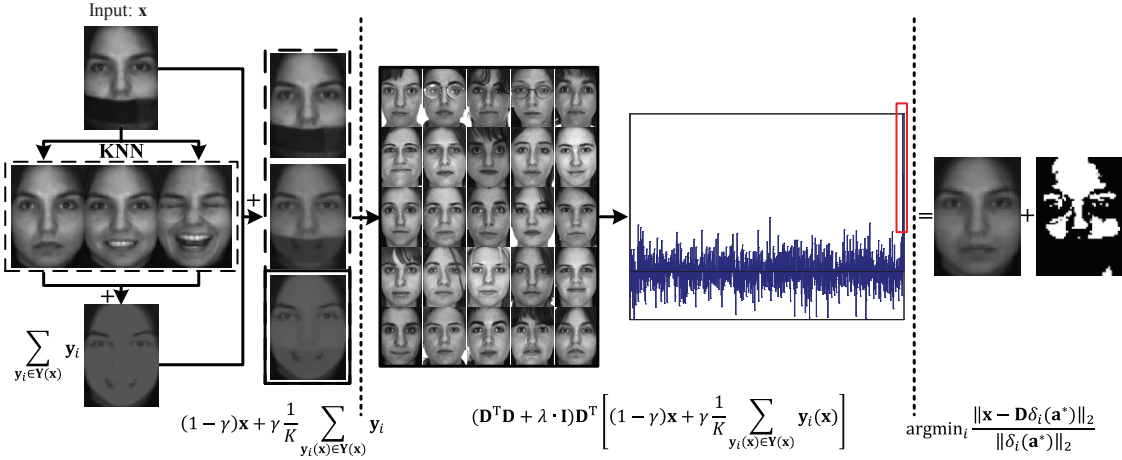


Figure 2: Overview of the coding process of LCCR, which consists of three steps separated by dotted lines. First, for a given input \mathbf{x} , find its neighborhood $\mathbf{Y}(\mathbf{x})$ from training data. Then, code \mathbf{x} over \mathbf{D} by finding the optimal representation \mathbf{a} (see bar graph) which produces the minimal reconstruction errors for \mathbf{x} and $\mathbf{Y}(\mathbf{x})$ simultaneously. Finally, conduct classification by finding which class produces the minimum residual. In the middle part of the figure, we use a red rectangles to indicate the basis vectors which produce the minimum residual.

2.2. ℓ^2 -minimization based methods

In [19], Naseem et al. proposed a Linear Regression Classifier (LRC) which achieved comparable accuracy to SRC in the context of robust face recognition. In another independent work[17], Shi et al. used the same objective function with that of LRC to discuss the role of ℓ^1 -regularization based sparsity. The objective function used in [19, 17] is

$$\operatorname{argmin}_{\mathbf{a}} \|\mathbf{x} - \mathbf{D}\mathbf{a}\|_2^2.$$

In [17], Shi et al. empirically showed that their method (denoted as LRC in this paper for convenience) requires \mathbf{D} to be an over-determined matrix for achieving competitive results, while the dictionary \mathbf{D} of SRC must be under-determined according to compressive sensing theory. Once the optimal code \mathbf{a}^* is calculated for a given input, the classifier (1) and (2) is used to determine the label for the input \mathbf{x} .

As another recent ℓ^2 -norm model, CRC-RLS [18] estimates the representation \mathbf{a}^* for the input \mathbf{x} by relaxing the ℓ^1 -norm to the ℓ^2 -norm in $P_{1,3}$. They aimed to solve following objective function:

$$\operatorname{argmin}_{\mathbf{a}} \|\mathbf{x} - \mathbf{D}\mathbf{a}\|_2^2 + \lambda \|\mathbf{a}\|_2^2,$$

where $\lambda > 0$ is a balance factor.

LRC and CRC-RLS show that ℓ^2 -norm based data models can achieve competitive classification accuracy with hundreds of times speed increase, compared with SRC. Under this background, we aim to incorporate the local geometric structures into coding process for achieving better discrimination and robustness.

3. Locality-Constrained Collaborative Representation

It is a big challenge to improve the discrimination and the robustness of facial representation because a practical face recognition system requires not only a high recognition rate but also the robustness against various noise and occlusions.

3.1. Algorithm Description

As two of the most promising methods, locality preservation based algorithm and sparse representation have been extensively studied and successfully applied to appearance-based face recognition, respectively. Locality preservation based algorithm aims to find a low-dimensional model by learning and preserving some properties shared by nearby

113 points from the original space to another one. Alternatively, sparse representation, which encodes each testing sample
 114 as a linear combination of the training data, depicts a global relationship between testing sample with training ones.
 115 In this paper, we aim to propose and formulate a kind of local consistency into coding scheme for modeling facial
 116 data. Our objective function is in the form of

$$117 \quad E(\mathbf{x}, \mathbf{a}) = \|\mathbf{x} - \mathbf{D}\mathbf{a}\|_2^2 + \lambda\|\mathbf{a}\|_p + \gamma E_L, \quad (3)$$

118 where $p = \{1, 2\}$, E_L is the locality constraint, $\lambda \geq 0$ and $\gamma \geq 0$ dictate the importance of $\|\cdot\|_p$ and E_L , respectively.
 119 Then the key is to formulate the shared property of the neighborhood with E_L .

120 E_L could be defined as the reconstruction error of the neighborhood of the testing image, i.e.,

$$121 \quad E_L(\mathbf{Y}(\mathbf{x}), \mathbf{C}) = \frac{1}{K} \sum_{\substack{\mathbf{y}_i(\mathbf{x}) \in \mathbf{Y}(\mathbf{x}) \\ \mathbf{c}_i \in \mathbf{C}}} \|\mathbf{y}_i(\mathbf{x}) - \mathbf{D}\mathbf{c}_i\|_2^2, \quad (4)$$

122 where, for an input $\mathbf{x} \in \mathbb{R}^M$, its neighborhood $\mathbf{Y}(\mathbf{x}) \in \mathbb{R}^{M \times K}$ is searched from the training samples according to prior
 123 knowledge or manual labeling. For simplicity, we assume that each data point has K neighbors, and $\mathbf{c}_i \in \mathbb{R}^N$ denotes
 124 the optimal code for $\mathbf{y}_i(\mathbf{x})$.

125 To bridge the connection between the objective variants \mathbf{a} and \mathbf{c}_i , it is possible to assume that \mathbf{a} could be denoted
 126 as a linear combination of $\{\mathbf{c}_i\}_{i=1}^K$. Mathematically,

$$127 \quad \mathbf{a} = \sum_{\mathbf{c}_i \in \mathbf{C}} w_i \mathbf{c}_i, \quad (5)$$

128 where w_i is the representation coefficient between \mathbf{a} and \mathbf{c}_i . The calculation of w_i is a challenging and key step which
 129 has been studied in many works. For example, Roweis and Saul [26] defined \mathbf{w} as the reconstruction coefficients over
 130 the nearby points in the original space. However, the approach is not suitable for our case since we aim to denote \mathbf{c}_i
 131 with \mathbf{a} but vice versa.

132 Motivated by a biological experiment of Ohki [29] as discussed in Section 1, we present a simple but effective
 133 method to solve the problem by directly replacing \mathbf{c}_i with \mathbf{a} . It is based on an observation (Figure 1) that the represen-
 134 tation of \mathbf{x} also can approximate the representation of \mathbf{y}_i , i.e.,

$$135 \quad \|\mathbf{y}_i - \mathbf{D}\mathbf{c}_i\|_2^2 \leq \|\mathbf{y}_i - \mathbf{D}\mathbf{a}\|_2^2 \leq \|\mathbf{y}_i - \mathbf{D}\bar{\mathbf{a}}\|_2^2,$$

136 where $\bar{\mathbf{a}}$ denotes the representation of the point which is not close to \mathbf{y}_i .

137 Thus, the proposed objective function is as follows:

$$138 \quad E(\mathbf{x}, \mathbf{Y}(\mathbf{x}), \mathbf{a}) = (1 - \gamma)\|\mathbf{x} - \mathbf{D}\mathbf{a}\|_2^2 + \gamma \frac{1}{K} \sum_{\mathbf{y}_i(\mathbf{x}) \in \mathbf{Y}(\mathbf{x})} \|\mathbf{y}_i - \mathbf{D}\mathbf{a}\|_2^2 + \lambda\|\mathbf{a}\|_p, \quad (6)$$

139 where $0 \leq \gamma \leq 1$ balances the importance between the testing image \mathbf{x} and its neighborhood $\mathbf{Y}(\mathbf{x})$. The second
 140 term, which measures the contribution of locality, can largely improve the robustness of \mathbf{a} . If \mathbf{x} is corrupted by noise
 141 or occluded by disguise, a larger γ will yield better recognition results.

142 On the other hand, the locality constraint in (6) is a simplified model of the property that similar inputs having
 143 similar codes. We think this might be a new interesting way to learn local consistency.

144 Consider the recent findings, i.e., ℓ^1 -norm based sparsity cannot bring a higher recognition accuracy and better
 145 robustness for facial data than ℓ^2 -norm based methods [17, 18], we simplify our objective function (6) as follows:

$$146 \quad E(\mathbf{x}, \mathbf{Y}(\mathbf{x}), \mathbf{a}) = (1 - \gamma)\|\mathbf{x} - \mathbf{D}\mathbf{a}\|_2^2 + \gamma \frac{1}{K} \sum_{\mathbf{y}_i(\mathbf{x}) \in \mathbf{Y}(\mathbf{x})} \|\mathbf{y}_i(\mathbf{x}) - \mathbf{D}\mathbf{a}\|_2^2 + \lambda\|\mathbf{a}\|_2^2. \quad (7)$$

147 Clearly, (7) achieves the minimum when its derivative with respect to \mathbf{a} is zero. Hence, the optimal solution is

$$148 \quad \mathbf{a}^* = (\mathbf{D}^T \mathbf{D} + \lambda \cdot \mathbf{I})^{-1} \mathbf{D}^T \left[(1 - \gamma)\mathbf{x} + \gamma \frac{1}{K} \sum_{\mathbf{y}_i(\mathbf{x}) \in \mathbf{Y}(\mathbf{x})} \mathbf{y}_i(\mathbf{x}) \right]. \quad (8)$$

Let $\mathbf{P} = (\mathbf{D}^T \mathbf{D} + \lambda \cdot \mathbf{I})^{-1} \mathbf{D}^T$ whose calculation requires re-formulating the psuedo-inverse, it can be calculated in advance and only once as it is only dependent on training data \mathbf{D} .

Given a testing image \mathbf{x} , the first step is to determine its neighborhood $\mathbf{Y}(\mathbf{x})$ from the training set according to prior knowledge, or manual labeling, etc. In practical applications, there are two widely-used variations for finding the neighborhood:

1. ϵ -ball method: The training sample \mathbf{d}_i is a neighbor of the testing image \mathbf{x} if $\|\mathbf{d}_i - \mathbf{x}\|_2 < \epsilon$, where $\epsilon > 0$ is a constant.
2. K -nearest neighbors (K -NN) searching: The training sample \mathbf{d}_i is a neighbor of \mathbf{x} , if \mathbf{d}_i is among the K -nearest neighbors of \mathbf{x} , where $K > 0$ can be specified as a constant or determined adaptively.

Once the neighborhood of the testing image \mathbf{x} is obtained, LCCR just simply projects \mathbf{x} and its neighborhood $\mathbf{Y}(\mathbf{x})$ onto space \mathbf{P} via (8). In addition, the matrix form of LCCR is easily derived, which can be used in batch prediction.

$$\mathbf{A}^* = (\mathbf{D}^T \mathbf{D} + \lambda \cdot \mathbf{I})^{-1} \mathbf{D}^T \left[(1 - \gamma) \mathbf{X} + \gamma \frac{1}{K} \sum_{i=1}^K \mathbf{Y}_i(\mathbf{X}) \right],$$

where the columns of $\mathbf{X} \in \mathbb{R}^{M \times J}$ are the testing images whose codes are stored in $\mathbf{A}^* \in \mathbb{R}^{N \times J}$, and $\mathbf{Y}_i(\mathbf{X}) \in \mathbb{R}^{M \times J}$ denotes the collection of i th-nearest neighbor of \mathbf{X} .

The proposed LCCR algorithm is summarized in Algorithm 1, and an overview is illustrated in Figure 2.

Algorithm 1 Face Recognition using Locality-Constrained Collaborative Representation (LCCR)

Input: A matrix of training samples $\mathbf{D} = [\mathbf{d}_1, \mathbf{d}_2, \dots, \mathbf{d}_N] \in \mathbb{R}^{M \times N}$ which are sorted according to the label of \mathbf{d}_i , $1 \leq i \leq N$; A testing image $\mathbf{x} \in \mathbb{R}^M$; The balancing factors $\lambda \geq 0$, $0 \leq \gamma \leq 1$, and the size of neighborhood K .

- 1: Normalize the columns of \mathbf{D} and \mathbf{x} to have a unit ℓ^2 -norm, respectively.
- 2: Calculate the projection matrix $\mathbf{P} = (\mathbf{D}^T \mathbf{D} + \lambda \cdot \mathbf{I})^{-1} \mathbf{D}^T$ and store it.
- 3: Find the neighborhood $\mathbf{Y}(\mathbf{x}) = \{\mathbf{y}_1(\mathbf{x}), \mathbf{y}_2(\mathbf{x}), \dots, \mathbf{y}_K(\mathbf{x})\}$ for \mathbf{x} from the training samples \mathbf{D} .
- 4: Code \mathbf{x} over \mathbf{D} via

$$\mathbf{a}^* = \mathbf{P} \cdot \left[(1 - \gamma) \mathbf{x} + \gamma \frac{1}{K} \sum_{\mathbf{y}_i(\mathbf{x}) \in \mathbf{Y}(\mathbf{x})} \mathbf{y}_i(\mathbf{x}) \right].$$

- 5: Compute the regularized residuals over all classes by

$$r_i(\mathbf{x}) = \frac{\|\mathbf{x} - \mathbf{D} * \delta_i(\mathbf{a}^*)\|_2}{\|\delta_i(\mathbf{a}^*)\|_2},$$

where i denotes the index of class.

Output: $\text{identity}(\mathbf{x}) = \text{argmin}_i \{r_i(\mathbf{x})\}$.

3.2. Discussions

From the algorithm, it is easy to see that the performance of LCCR is positively correlated with that of K -NN searching method. Thus, it is possible to assume that LCCR will be failed if K -NN cannot find the correct neighbors for the testing sample. Here, we give a real example (Figure3) to illustrate that LCCR would largely avoid such situations from happening. In the example, the classification accuracy of LCCR is about 94% by using 600 AR images with sunglasses as testing image and 1400 clean ones as training samples.

Figure 3(a) demonstrates the coefficients and residual of LCCR and CRC-RLS. We can see that the two methods correctly predicted the identity of the input, while K -NN searching could not find the correct neighbors (see Figure 3(b)). It illustrates that LCCR could work well even though K -NN is failed to get the results. Figure 3(c) and Figure 3(d) illustrate another possible case. That is, CRC-RLS fails to get the correct identity of the input while the nearest neighbor comes from the 7th individual, and LCCR successfully obtains the the correct identify.

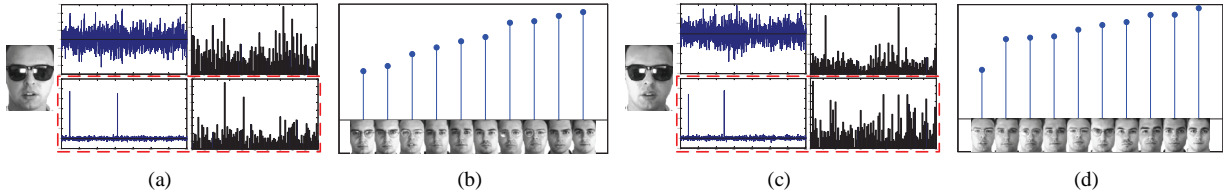


Figure 3: The effectiveness of the proposed model. (a) A testing face disguised by sunglasses comes from the 7th subject of AR database. The figures (in the red rectangle) in the second row are the coefficients and residual of the input learned by LCCR ($\lambda = 0.005$, $\gamma = 0.9$, and $k = 2$); the figures in the first row are the results of CRC-RLS [18] ($\lambda = 0.001$ for the best accuracy). (b) The 10 nearest neighbors of the input in terms of cityblock distance (Y-axis). (c) and (d) are the results of another testing sample from the same individual.

3.3. Computational Complexity Analysis

The computational complexity of LCCR consists of two parts for offline and online computation, respectively. Suppose the dictionary \mathbf{D} contains n samples with m dimensionality, LCCR takes $O(mn^2 + n^3)$ to compute the projection matrix $(\mathbf{D}^T \mathbf{D} + \lambda \mathbf{I})^{-1} \mathbf{D}^T$ and $O(mn)$ to store it.

For each querying sample \mathbf{y} , LCCR needs $O(mn)$ to search the K -nearest neighbors of \mathbf{y} from \mathbf{D} . After that, the algorithm projects \mathbf{y} into another space via (8) in $O(m^2n)$. Thus, the computational complexity of encoding LCCR is $O(m^2n)$ for each unknown sample. Note that, the computational complexity of LCCR is same with that of LRC [17, 19] and CRC-RLS [18], and it is more competitive than SRC [10] even though the fastest ℓ^1 -solver is used. For example, SRC takes $O(t_1 m^2 n + t_1 m n^2)$ to code each sample over \mathbf{D} when Homotopy optimizer [31] is adopted to get the sparsest solution, where Homotopy optimizer is one of the fastest ℓ^1 -minimization algorithm according to [5] and t denotes the number of iterations of Homotopy algorithm. From the above analysis, it is easy to find that a medium-sized data set will bring up the scalability issues with the models. To address the problem, a potential choice is to perform dimension reduction or sampling techniques to reduce the size of problem in practical application as did in [32].

4. Experimental Verification and Analysis

In this section, we report the performance of LCCR over four publicly-accessed facial databases, i.e., AR [33], ORL [34], the Extended Yale database B [35], and Multi-PIE [36]. We examine the recognition results of the proposed algorithm with respect to 1) discrimination, 2) robustness to corruptions, 3) and robustness to occlusions.

4.1. Experimental Configuration

We compared the classification results of LCCR with four linear coding models (SRC [10], CESR [13], LRC [17, 19] and CRC-RLS [18]) and a subspace learning algorithm (LPP [30]) with the nearest neighbors classifier (INN). Moreover, we also reported the results of linear SVM [37] over the original inputs. Note that, SRC, CESR, LRC, CRC-RLS and LCCR directly code each testing sample over training data without usability of dictionary learning method, and get classification result by finding which subject produces the minimum reconstruction error. In these models, only LCCR incorporates locality based pairwise distance into coding scheme. For a comprehensive comparison, we report the performance of LCCR with five basic distance metrics, i.e., Euclidean distance (ℓ^2 -distance), Seucclidean distance (standardized Euclidean distance), Cosine distance (the cosine of the angle between two points), Cityblock distance (ℓ^1 -distance), and Spearman distance.

For computational efficiency, as did in [10, 18], we performed Eigenface [38] to reduce the dimensionality of data set throughout the experiments. Moreover, SRC requires the dictionary \mathbf{D} to be an under-determined matrix, and Shi et al. [17] claimed that their model (named as LRC in [19]) will achieve competitive results when \mathbf{D} is over-determined. For a extensive comparison, we investigate the performance of the tested methods except SRC over two cases.

We solved the ℓ^1 -minimization problem in SRC by using the CVX [39], a package for solving convex optimization problems, and got the results of LRC, CRC-RLS and CESR by using the source codes from the homepages of the authors. All experiments are carried out using Matlab 32bit on a 2.5GHz machine with 2.00 GB RAM.

Parameter determination is a big challenge in pattern recognition and computer vision. As did in [7, 6], we report the best classification results of all tested methods under different parameter configurations. The value range used to

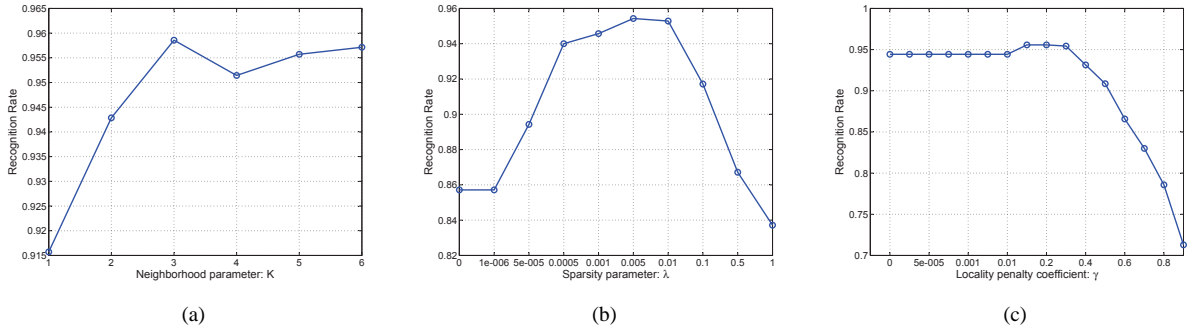


Figure 4: Recognition accuracy of LCCR using Cityblock distance on a subset of AR database with dimensionality 2580. (a) The recognition rates versus the variation of the neighborhood parameter K , where $\lambda = 0.005$ and $\gamma = 0.2$. (b) The recognition rates versus the variation of the sparsity parameter λ , where $K = 5$ and $\gamma = 0.2$. (c) The recognition rates versus the variation of the locality constrained coefficient γ , where $K = 3$ and $\lambda = 0.005$.

Table 1: The Maximal Recognition Accuracy of Competing Algorithms on the ORL Database.

Dim	54	120	200	2688
SVM [37]	90.00%	92.50%	93.50%	93.00%
LPP [30]	86.00%	86.50%	86.50%	86.50%
SRC [10]	92.00%	96.50%	86.00%	-
CESR [13]	89.50%	88.50%	89.00%	97.50%
LRC [17, 19]	92.50%	91.00%	89.00%	89.00%
CRC-RLS [18]	94.50%	94.00%	94.50%	95.00%
LCCR + Cityblock	97.50%	97.50%	98.00%	98.00%
LCCR + Seuclidean	96.00%	96.50%	96.00%	96.50%
LCCR + Euclidean	96.00%	96.00%	96.50%	96.50%
LCCR + Cosine	96.00%	96.50%	96.50%	96.50%
LCCR + Spearman	96.00%	96.00%	96.00%	96.00%

211 find the best values for LCCR can be inferred from Figure 4, and these possible values of λ also are tested for SRC
 212 and CRC-RLS. In all tests, we randomly split each data set into two parts for training and testing, and compare the
 213 performance of the algorithms using the same partition to avoid the difference in data sets.

214 4.2. Recognition on Clean Images

215 In this sub-section, we examine the performance of 7 competing methods over 4 clean facial data sets. Here, clean
 216 image means an image without occlusion or corruption, just with variations in illumination, pose, expression, etc.

217 (1) **ORL database** [34] consists of 400 different images of 40 individuals. For each person, there are 10 images
 218 with the variation in lighting, facial expression and facial details (with or without glasses). For computational effi-
 219 ciency, we cropped all ORL images from 112×96 to 56×48 , and randomly selected 5 images from each subject for
 220 training and used the remaining 5 images for testing.

221 Table 1 reports the classification accuracy of the tested algorithms over various dimensionality. Note that, the
 222 Eigenface with 200D retains 100% energy of the cropped data, which makes the investigated methods achieve the
 223 same rates over 2688D. From the results, LCCRs outperform the other algorithms, and the best results are achieved
 224 when Cityblock distance is used to search the nearest neighbors. Moreover, we can find that all the algorithms achieve
 225 a higher recognition rate in the original space except LRC. One possible reason is that the cropped operation degrades
 226 the performance of LRC, another reason may attribute to the used classifier. Moreover, we have found that if another
 227 nearest subspace classifier [10] is adopted with linear regression based representation, the accuracy of LRC is slightly
 228 decreased from 89% to 88.00% over the original data and from 91% to 90% with 120D.

229 (2) **AR database** [33] includes over 4000 face images of 126 people (70 male and 56 female) which vary in
 230 expression, illumination and disguise (wearing sunglasses or scarves). Each subject has 26 images consisting of 14
 231 clean images, 6 images with sunglasses and 6 images with scarves. As did in [10, 18], a subset that contains 1400
 232 normal faces randomly selected from 50 male subjects and 50 female subjects, is used in our experiment. For each
 233 subject, we randomly permute the 14 images and take the first half for training and the rest for testing. Limited by the

Table 2: The Maximal Recognition Accuracy of Competing Algorithms on the AR Database.

Dim	54	120	300	2580
SVM [37]	73.43%	81.00%	82.00%	83.14%
LPP [30]	39.29%	43.57%	53.86%	53.86%
SRC [10]	81.71%	88.71%	90.29%	-
CESR [13]	74.00%	81.43%	84.57%	84.57%
LRC [17, 19]	80.57%	90.14%	93.57%	82.29%
CRC-RLS [18]	80.57%	90.43%	94.00%	94.43%
LCCR + Cityblock	86.14%	92.71%	95.14%	95.86%
LCCR + Seclidean	85.00%	91.86%	94.43%	95.43%
LCCR + Euclidean	84.00%	91.29%	94.14%	94.86%
LCCR + Cosine	83.43%	90.86%	94.00%	94.57%
LCCR + Spearman	84.71%	90.71%	94.14%	94.43%

Table 3: The Maximal Recognition Accuracy of Competing Algorithms on the Extended Yale B Database.

Dim	54	120	300	2592
SVM [37]	84.52%	92.72%	95.28%	95.45%
LPP [30]	35.93%	54.55%	70.78%	75.66%
SRC [10]	93.71%	95.12%	96.44%	-
CESR [13]	92.30%	94.95%	95.53%	96.11%
LRC [17, 19]	92.88%	95.61%	97.85%	90.48%
CRC-RLS [18]	92.96%	95.69%	97.90%	98.26%
LCCR + Cityblock	93.21%	96.03%	97.93%	98.34%
LCCR + Seclidean	93.21%	95.70%	97.93%	98.34%
LCCR + Euclidean	93.21%	95.70%	97.93%	98.34%
LCCR + Cosine	93.46%	95.78%	97.93%	98.59%
LCCR + Spearman	97.02%	98.18%	99.10%	99.59%

computational capabilities, as in [18], we crop all images from original 165×120 to 60×43 (2580D) and convert it to gray scale.

(3) **Extended Yale B database** [35] contains 2414 frontal-face images with size 192×168 over 38 subjects, as did in [10, 18], we carried out the experiments on the cropped and normalized images of size 54×48 . For each subject (about 64 images per subject), we randomly split the images into two parts with equal size, one for training, and the other for testing. Similar to the above experimental configuration, we calculated the recognition rates over dimensionality 54, 120 and 300 using Eigenface, and 2592D in the original data space. Table 3 show that LCCRs again outperform its counterparts across various spaces, especially when the Spearman distance is used to determine the neighborhood of testing samples.

(4) **Multi PIE database** (MPIE) [36] contains the images of 337 subjects captured in 4 sessions with simultaneous variations in pose, expression and illumination. As did in [18], we used all the images in the first session as training data and the images belonging to the first 250 subjects in the other sessions as testing data. All images are cropped from 100×82 to 50×41 .

From Tables 1-4, we draw the following conclusions:

1. LCCRs generally outperforms SVM (original input), SRC (sparse representation), CESR (robust sparse representation), LRC (linear regression based model) and CRC-RLS (collaborative representation) over the tested cases.
2. LCCRs perform better in a low-dimensional space than a high-dimensional ones. For example, on the Extended Yale B, the difference in accuracy between LCCR and CRC-RLS (the second best method) changed from 4.06% (54D) to 2.49% (120D) and to 1.17% (300D). It again corroborates our claim that local consistency is helpful to improving the discrimination of data representation, since the low-dimensional data contain few information than higher one.
3. CESR is more competitive in the original space at the cost of computing cost. For example, it outperforms the other models over MPIE-S4 in classification accuracy where its time cost about 11003.51 seconds, compared with 3104.82s of SRC, 54.59s of LRC, 54.79s of CRC-RLS and 59.82s of LCCR.
4. SRC, LRC and CRC-RLS achieve the similar performance, and SRC is more competitive in the low-dimensional feature spaces. The results are consistent with the reports in [18]. For example, in the experiments of Zhang over MPIE-S2 with 300D, the accuracy scores of SRC and CRC-RLS are about 93.9% and 94.1%, respectively, comparing with 93.13% and 94.88% in our experiments. Moreover, CRC-RLS and LRC achieve similar

Table 4: The Maximal Recognition Accuracy of Competing Algorithms on the Multi PIE database.

Dim	300			2050		
	MPIE-S2	MPIE-S3	MPIE-S4	MPIE-S2	MPIE-S3	MPIE-S4
SVM [37]	91.33%	85.13%	89.20%	91.45%	85.75%	89.43%
LPP [30]	40.12%	27.44%	31.20%	31.49%	31.00%	31.49%
SRC [10]	93.13%	90.60%	94.10%	-	-	-
CESR [13]	92.41%	87.38%	91.94%	94.46%	92.06%	96.17%
LRC [17, 19]	94.64%	89.88%	93.37%	83.19%	70.25%	75.03%
CRC-RLS [18]	94.88%	89.88%	93.60%	95.30%	90.56%	94.46%
LCCR + Cityblock	95.36%	91.25%	95.54%	96.08%	91.94%	95.89%
LCCR + Seucclidean	95.06%	91.25%	94.51%	95.84%	91.56%	95.20%
LCCR + Euclidean	95.06%	91.31%	94.57%	95.84%	91.63%	95.14%
LCCR + Cosine	95.12%	90.88%	94.69%	95.78%	91.38%	95.14%
LCCR + Spearman	95.12%	91.75%	94.40%	95.78%	92.19%	95.20%



(a)

Features	Right Eye	Mouth and Chin	Nose
Dim	308	798	224
SVM [37]	70.71%	41.29%	37.14%
LPP [30]	58.57%	14.43%	53.71%
SRC [10]	84.00%	70.71%	78.00%
CESR [13]	81.57%	56.00%	70.43%
LRC [17, 19]	72.86%	32.86%	70.57%
CRC-RLS [18]	83.14%	73.86%	73.57%
LCCR + Cityblock	86.86%	76.29%	75.86%
LCCR + Seucclidean	84.86%	75.57%	75.29%
LCCR + Euclidean	85.29%	75.00%	76.00%
LCCR + Cosine	84.43%	74.57%	75.29%
LCCR + Spearman	84.57%	75.86%	75.14%

(b)

Figure 5: Recognition Accuracy with partial face features. (a) An example of the three features, right eye, mouth and chin, and nose from left to right. (b) The recognition rates of competing methods on the partial face features of the AR database.

263 recognition rates with the difference less than 1% across various feature spaces.

264 4.3. Recognition on Partial Facial Features

265 The ability to work on partial face features is very interesting since not all facial features play an equal role in
 266 recognition. Therefore, this ability has become an important metric in the face recognition researches [40]. We
 267 examine the performance of the investigated methods using three partial facial features, i.e., right eye, nose, as well as
 268 mouth and chin, sheared from the clean AR faces with 2580D (as shown in Figure 5(a)). For each partial face feature,
 269 we generate a data set by randomly selecting 7 images per subject for training and the remaining 700 for testing. It
 270 should be noted that [10] conducted the similar experiment on Extended Yale B which includes less subjects, smaller
 271 irrelevant white background, and more training samples per subject than our case.

272 Figure 5(b) shows that LCCRs achieve better recognition rates than SVM, SRC, LRC and CRC-RLS for right eye
 273 as well as mouth and chin, and the second best rates for the nose. Some works found that the most important feature is
 274 the eye, followed by the mouth, and then the nose [41]. We can see that the results for SVM, CRC-RLS and LCCR are
 275 consistent with the conclusions even though the dominance of the mouth and chin over the nose is not very distinct.

276 4.4. Face Recognition with Block Occlusions

277 To examine the robustness to block occlusion, similar to [10, 17, 18], we get 700 testing images by replacing a
 278 random block of each clean AR image with an irrelevant image (baboon) and use 700 clean images for training. The
 279 occlusion ratio increases from 10% to 50%, as shown in Figure 6(a). We investigate the classification accuracy of the
 280 methods across Eigenface space with 300D (Figure 6(b)) and cropped data space with 2580D (Figure 6(c)).

281 Figures 6(b)-6(d) show that LCCRs generally outperform the other models with considerable performance mar-
 282 gins. Especially, with the increase of the occlusion ratio, the difference in recognition rates of LCCRs and the other
 283 methods becomes larger. For example, when the occlusion ratio is 50%, in 300 dimensional space, the accuracy of
 284 LCCR with Cityblock distance is about 19.7% higher than SVM, about 44.1% higher than LPP, about 26.0% higher

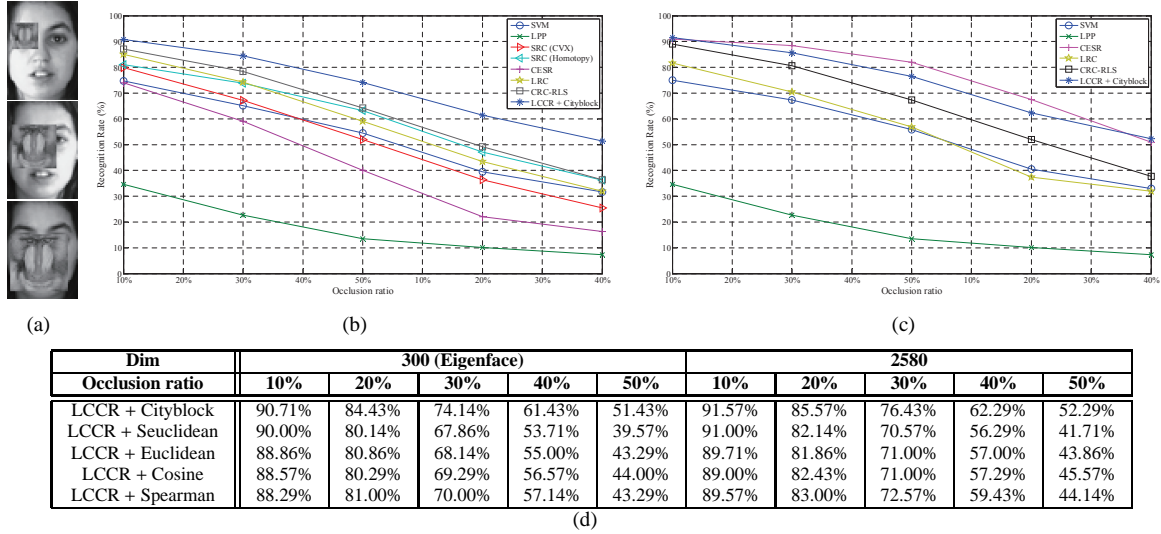


Figure 6: Experiments on AR database with varying percent block occlusion. (a) From top to bottom, the occlusion percents for test images are, 10%, 30%, and 50%, respectively. (b) and (c) are the recognition rates under different levels of block occlusion on AR database with 300D (Eigenface) and 2580D, respectively. (d) The recognition rates of LCCRs with 300D and 2580D.

285 than SRC (CVX), about 35.1% higher than CESR, about 19.6% higher than LRC, and about 15.1% higher than CRC-
 286 RLS. Note that, different ℓ^1 -solvers will lead to different results for SRC. For Example, if SRC adopts Homotopy
 287 algorithm [31] to get the sparsest solution, the recognition rate will increase from 25.43% (with CVX) to 36.14% such
 288 that the performance dominance decreases from 26% to 15.3%. Moreover, CESR achieves the best results at the cost
 289 of computational cost when the original data is available and the occluded ratio ranges from 20% to 40%.

290 On the other hand, it is easy to find that LRC, CRC-RLS and LCCRs are more robust than SRC and SVM, which
 291 implies that the ℓ^1 -regularization term cannot yield better robustness than the ℓ^2 -regularization term, at least for the
 292 Eigenface space. Moreover, the models achieve better results in higher dimensional space, even though the difference
 293 of classification accuracy between higher dimensional space and lower ones is less than 1% except CESR has an
 294 obvious improvement.

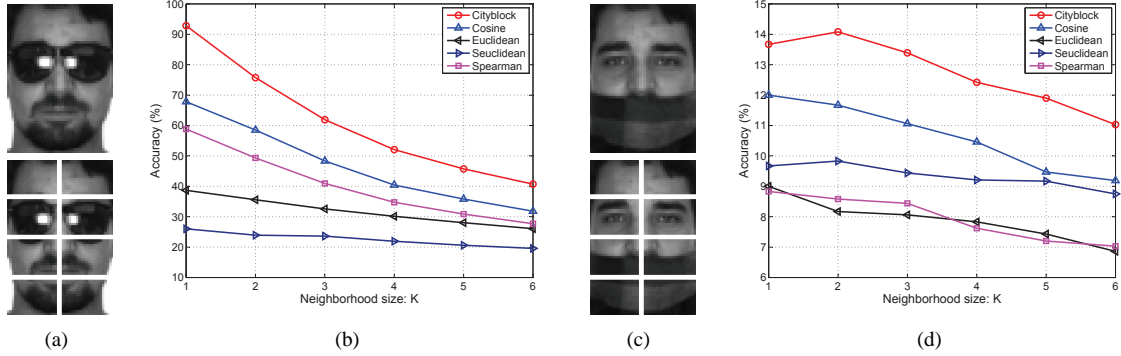
295 4.5. Face Recognition with Real Occlusions

296 In this sub-section, we examine the robustness to real possible occlusions of the investigated approaches over the
 297 AR data set. We use 1400 clean images for training, 600 faces wearing by sunglasses (occluded ratio is about 20%)
 298 and 600 face wearing by scarves (occluded ratio is about 40%) for testing, separately. In [10], Wright et al. only used
 299 a third of disguised images for this test, i.e., 200 images for each kind of disguises. In addition, we also investigate
 300 the role of K -NN searching in LCCR.

301 We examine two widely-used feature schemes, namely, the holistic feature with 300D and 2580D, as well as
 302 the partitioned feature based on the cropped data. The partitioned feature scheme firstly partitions an image into
 303 multiple blocks (8 blocks as did in [10, 18, 28], see Figure 7(a) and 7(c)), then conducts classification on each block
 304 independently, and after that, aggregates the results by voting.

305 Figure 7(e) reports the recognition rates of all the tested methods. For the images occluded by sunglasses, LCCR
 306 with Cityblock distance and CESR achieve remarkable results with the holistic feature scheme, their recognition accu-
 307 racy are nearly double that of the other methods. This considerable performance margin contributes to the accuracy
 308 of K -NN searching based on Cityblock distance (see Figure 7(b)).

309 For the images occluded by scarves, LCCR achieves the highest recognition rate over the full dimensional space,
 310 and the second highest rates using Eigenface. However, the difference in rates between LCCR and other non-iterative
 311 algorithms (LRC, CRC-RLS) is very small due to the poor accuracy of K -NN searching as shown in Figure 7(d).
 312 Furthermore, the partitioned feature scheme produces higher recognition rates than the holistic one for all competing
 313 methods, which is consistent with previous report [10].



Disguise Feature Dim	sunglasses			scarves		
	Holistic		Partitioned	Holistic		Partitioned
	300	2580	2580	300	2580	2580
SVM [37]	47.83%	48.67%	40.17%	13.50%	13.83%	41.67%
LPP [30]	14.83%	18.50%	88.83%	20.33%	24.17%	82.00%
SRC [10]	57.00%	-	93.00%	69.83%	-	91.83%
CESR [13]	21.17%	95.50%	97.50%	31.50%	16.67%	91.33%
LRC [17, 19]	52.83%	49.17%	88.17%	68.50%	57.50%	91.83%
CRC-RLS [18]	53.00%	71.50%	88.33%	68.50%	89.17%	92.17%
LCCR + Cityblock	93.00%	93.50%	91.17%	68.67%	89.17%	92.50%
LCCR + Seucclidean	57.83%	74.50%	91.50%	68.50%	89.17%	92.17%
LCCR + Euclidean	66.00%	79.00%	90.83%	68.67%	89.17%	92.50%
LCCR + Cosine	76.83%	85.33%	93.83%	68.83%	89.50%	93.83%
LCCR + Spearman	70.67%	81.17%	95.83%	68.67%	89.33%	93.83%

(e)

Figure 7: Recognition on AR faces with real possible occlusions. (a) The top row is a facial image occluded by sunglasses, whose partitioned blocks are shown as below. (b) The accuracy of K -NN searching using Cityblock distance, Cosine distance, Euclidean distance, Seucclidean distance and Spearman distance on the AR images with sunglasses (2580D). (c) Similar to (a), the top row is a face occluded by scarf, and its partitions below. (d) The precision of K -NN searching using Cityblock, Cosine, Euclidean, Seucclidean, Spearman as distance metrics on the AR images with scarves (2580D). (e) The recognition rates of competing methods across different experimental configurations.

314 From the above experiments, it is easy to conclude that the preservation of locality is helpful to coding scheme,
315 especially when the real structures of data cannot be found by traditional coding scheme. Moreover, the performance
316 ranking of LCCR with five distance metrics is same with that of K -NN searching with the used metrics.

317 4.6. Face Recognition with Corruption

318 We test the robustness of LCCR against two kinds of corruption using the AR data set containing 2600 images
319 of 100 individuals. For each subject, we use 13 images for training (7 clean images, 3 images with sunglasses, and
320 3 images with scarves), and the remaining 13 images for testing. Different from [10] which tested the robustness to
321 corruption using the Extended Yale B database, our case is more challenging for the following reasons. Firstly, AR
322 images contain real possible occlusions, i.e., sunglasses and scarves, while Extended Yale B is a set of clean images
323 without disguises. Secondly, AR includes more facial variations (13 versus 9), more subjects (100 versus 38), and
324 a smaller samples for each subject (26 images per subject versus 64 images per subject). Thirdly, we investigated
325 two kinds of corruption, white noise (additive noise) and random pixel corruption (non-additive noise) which are two
326 commonly assumed in face recognition problem [10, 17, 19]. For the white noise case (the top row of Figure 8), we
327 add random noise from normal distribution to each testing image \mathbf{x} , that is, $\tilde{\mathbf{x}} = \mathbf{x} + \alpha \mathbf{n}$, and restrict $\tilde{\mathbf{x}} \in [0, 255]$, where
328 α is the corruption ratio from 10% to 90% with an interval of 20%, and \mathbf{n} is the noise following a standard normal
329 distribution. For the random pixel corruption case (the bottom row in Figure 8), we replace the value of a percentage
330 of pixels randomly chosen from each test image with the values following a uniform distribution over $[0, p_{max}]$, where
331 p_{max} is the largest pixel value of current image.

332 To improve the anti-noise ability of SRC [10], Wright et al. generate a new dictionary $[\mathbf{D} \ \mathbf{I}]$ by concatenating
333 an identity matrix \mathbf{I} with the original dictionary \mathbf{D} , where the dimensionality of \mathbf{I} equals to that of data. The use
334 of \mathbf{I} has been verified to be effective in improving the robustness of ℓ^1 -norm based models [42, 10] at the cost of

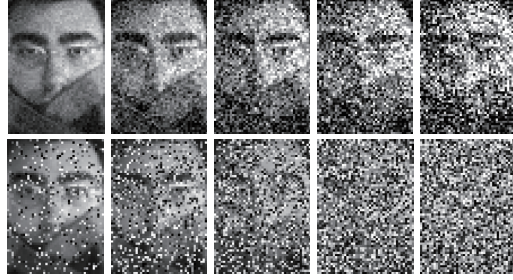


Figure 8: Testing images from AR database with additive noise and non-additive noise. Top row: 10%, 30%, 50%, 70%, 90% white noises are added into test image; Bottom row: the case of random pixel corruption with 10%-90% percentages, respectively.

Table 5: The Robustness of Different Methods over AR Database with 300D (Coding over \mathbf{D}).

Corruptions Corrupted ratio	White Gaussian Noise					Random Pixel Corruption				
	10%	30%	50%	70%	90%	10%	30%	50%	70%	90%
SVM [37]	91.77%	91.38%	90.23%	88.62%	82.69%	91.54%	81.92%	45.46%	8.23%	2.00%
LPP+1NN [30]	29.31%	8.46%	4.08%	2.38%	2.62%	5.69%	2.62%	2.00%	1.46%	1.17%
SRC [10]	92.62%	91.23%	86.54%	78.31%	62.62%	89.62%	72.31%	38.85%	8.23%	2.00%
CESR [13]	89.69%	87.85%	85.38%	80.85%	73.00%	87.38%	76.31%	43.23%	12.38%	1.46%
LRC [17, 19]	93.39%	92.39%	88.85%	81.85%	67.62%	91.77%	77.00%	45.77%	13.62%	2.54%
CRC-RLS [18]	94.77%	94.39%	92.85%	90.92%	87.31%	84.08%	88.69%	65.46%	20.77%	2.92%
LCCR + Cityblock	97.00%	96.00%	94.54%	92.31%	89.08%	96.54%	92.31%	79.69%	37.08%	5.23%
LCCR + Seclidean	96.31%	95.85%	94.46%	92.39%	88.54%	95.69%	90.08%	65.85%	20.77%	3.00%
LCCR + Euclidean	95.77%	95.23%	94.23%	92.31%	88.31%	95.39%	90.39%	67.23%	20.92%	3.23%
LCCR + Cosine	95.62%	95.31%	93.92%	92.15%	88.69%	94.85%	89.46%	65.62%	20.85%	3.69%
LCCR + Spearman	96.15%	95.39%	94.69%	93.08%	89.77%	95.54%	92.54%	83.00%	59.31%	13.69%

time-consuming. Therefore, it is a tradeoff between robustness and efficiency for the algorithms. Will the strategy still work for ℓ^2 -minimization based models? In this sub-section, we fill this gap by comparing the results by coding over these two dictionary.

Table 5 through Table 8 are the recognition rates of the tested methods across feature space (Eigenface with 300D) and full dimensional space (2580D). We didn't reported the results of SVM and LPP with the strategy of expanding dictionary since the methods are not belong to the facility of linear coding scheme. Moreover, SRC requires the dictionary is an over-completed matrix such that it could not run in the full dimensional cases. Based on the results, we have the following conclusions:

Firstly, the proposed LCCRs are much superior to SVM, LPP, SRC, CESR, LRC and CRC-RLS. For example, in the worst case (the white gaussian noise corruption ratio is 90%, the best result of LCCR is about 90.54% (Table 6), compared to 82.92% of SVM (Table 6), 2.62% of LPP (Table 5), 84.08% of SRC (Table 7), 73% of CESR (Table 5), 87.15% of LRC (Table 8), and 88.39% of CRC-RLS (Table 6). In the case of random pixel corruption, one can see when the corruption ratio reaches 70%, all methods fail to perform recognition except LCCR in the two data spaces and CESR in the full dimensional space.

Secondly, all investigated algorithms perform worse with increased corruption ratio and achieve better results in white noise corruption (additive noise) than random pixel corruption (non-additive noise). Moreover, the improvement of CESR is obvious when the original data is used to test. As discussed in the above, the improvement is at the cost of computational efficiency. For the other methods, they perform slightly better (less than 1%) in the full-dimensional space except LRC.

Thirdly, the results show that coding over $[\mathbf{D} \mathbf{I}]$ is helpful in improving the robustness of SRC and LRC, but it has negative impact on the recognition accuracy of CESR, CRC-RLS and LCCR. For example, when white noise ratio rises to 90% for the Eigenface (Table 5, expanding \mathbf{D} leads to the variation of the recognition rate from 62.62% to 84.08% for SRC, from 73.00% to 63.15% for CESR, from 67.62% to 86.31% for LRC, from 87.31% to 86.31% for CRC-RLS, and from 89.77% to 87.54% for LCCR with Spearman distance. The conclusion has not been reported in the previous works.

Table 6: The Robustness of Different Methods over AR Database with 2580D (Coding over \mathbf{D}).

Corruptions Corrupted ratio	White Gaussian Noise					Random Pixel Corruption				
	10%	30%	50%	70%	90%	10%	30%	50%	70%	90%
SVM [37]	91.92%	91.31%	89.85%	88.62%	82.92%	91.69%	81.46%	44.77%	7.69%	1.92%
LPP+1NN [30]	37.69%	10.31%	4.54%	3.00%	2.54%	6.92%	2.54%	2.15%	1.46%	1.47%
CESR [10]	90.85%	86.69%	84.38%	78.85%	70.08%	91.00%	90.77%	90.54%	66.08%	13.08%
LRC [17, 19]	78.69%	33.77%	4.62%	4.62%	2.69%	21.77%	3.77%	2.39%	0.92%	1.15%
CRC-RLS [18]	94.85%	94.77%	93.23%	90.85%	88.39%	94.15%	89.08%	67.08%	22.69%	2.62%
LCCR + Cityblock	97.54%	96.08%	95.08%	93.15%	90.54%	96.85%	93.23%	78.77%	29.77%	4.54%
LCCR + Seclidean	96.92%	96.23%	95.39%	92.92%	89.00%	96.00%	90.77%	67.31%	22.69%	3.00%
LCCR + Euclidean	96.08%	95.62%	94.85%	92.23%	88.92%	95.62%	91.15%	68.31%	22.92%	3.00%
LCCR + Cosine	96.08%	95.46%	94.39%	92.54%	89.46%	95.31%	90.77%	67.15%	23.23%	3.62%
LCCR + Spearman	96.54%	95.23%	94.69%	93.31%	90.39%	95.85%	92.92%	83.31%	60.69%	13.85%

Table 7: The Robustness of Different Methods over AR Database with 300D (Coding over $[\mathbf{D} \ \mathbf{E}]$).

Corruptions Corrupted ratio	White Gaussian Noise					Random Pixel Corruption				
	10%	30%	50%	70%	90%	10%	30%	50%	70%	90%
SRC [10]	92.62%	91.08%	90.46%	87.92%	84.08%	91.62%	83.38%	56.31%	14.92%	2.08%
CESR [13]	85.69%	82.46%	80.31%	73.69%	63.15%	83.38%	69.00%	34.69%	10.62%	2.92%
LRC [17, 19]	92.62%	92.15%	91.00%	88.85%	86.31%	91.15%	84.46%	49.92%	8.31%	1.85%
CRC-RLS [18]	92.62%	92.15%	91.00%	88.85%	86.31%	91.15%	84.46%	49.92%	8.31%	1.85%
LCCR + Cityblock	93.08%	92.39%	91.69%	89.62%	86.62%	92.62%	87.54%	69.46%	34.00%	4.92%
LCCR + Seclidean	92.85%	92.39%	91.69%	89.62%	86.46%	91.85%	85.23%	50.00%	8.31%	2.46%
LCCR + Euclidean	92.85%	92.39%	91.69%	89.92%	86.62%	91.92%	85.15%	51.23%	10.23%	2.54%
LCCR + Cosine	92.69%	92.69%	91.92%	89.92%	87.00%	92.15%	84.92%	49.92%	8.38%	2.62%
LCCR + Spearman	92.85%	92.85%	92.15%	90.15%	87.54%	92.69%	87.85%	75.92%	56.54%	1.38%

5. Conclusions and Discussions

It is interesting and important to improve the discrimination and robustness of data representation. The traditional coding algorithm gets the representation by encoding each datum as a linear combination of a set of training samples, which mainly depicts the global structure of data. However, it will be failed when the data are grossly corrupted. Locality (Local consistency) preservation, which keeps the geometric structure of manifold for dimension reduction, has shown the effectiveness in revealing the real structure of data. In this paper, we proposed a novel objective function to get an effective and robust representation by enforcing the similar inputs produce similar codes, and the function possesses analytic solution.

The experimental studies showed that the introduction of locality makes LCCR more accurate and robust to various occlusions and corruptions. We investigated the performance of LCCR with five basic distance metrics (for locality). The results imply that if better K -NN searching methods or more sophisticated distance metrics are adopted, LCCR might achieve a higher recognition rate. Moreover, the performance comparisons over two different dictionaries show that it is unnecessary to expand the dictionary \mathbf{D} with \mathbf{I} for ℓ^2 -norm based coding algorithms.

Each approach has its own advantages and disadvantages. Parameter determination maybe is the biggest problem of LCCR which requires three user-specified parameters. In the future works, it is possible to explore the relationship between locality parameter k and the intrinsic dimensionality of sub-manifold. Moreover, the work has focused on the representation learning, however, dictionary learning is also important and interesting in this area. Therefore, an possible way to extend this work is exploring how to reflect local consistency in the formation process of dictionary.

References

- [1] E. J. Candes, T. Tao, Decoding by linear programming, *IEEE Transactions on Information Theory* 51 (12) (2005) 4203–4215.
- [2] D. L. Donoho, For most large underdetermined systems of linear equations the minimal ℓ^1 -norm solution is also the sparsest solution, *Communications on Pure and Applied Mathematics* 59 (6) (2006) 797–829.
- [3] S. S. B. Chen, D. L. Donoho, M. A. Saunders, Atomic decomposition by basis pursuit, *SIAM Review* 43 (1) (2001) 129–159.
- [4] B. Efron, T. Hastie, I. Johnstone, R. Tibshirani, Least angle regression, *Annals of Statistics* 32 (2) (2004) 407–451.
- [5] A. Yang, A. Ganesh, S. Sastry, Y. Ma, Fast ℓ^1 -minimization algorithms and an application in robust face recognition: a review, in: *Proc. of International Conference on Image Processing*, 2010, pp. 1849–1852.
- [6] P. Xi, L. Zhang, Z. Yi., Constructing l2-graph for subspace learning and segmentation, *ArXiv e-prints* arXiv:1209.0841.
- [7] B. Cheng, J. Yang, S. Yan, Y. Fu, T. Huang, Learning with ℓ^1 -graph for image analysis, *IEEE Transactions on Image Processing* 19 (4) (2010) 858–866.

Table 8: The Robustness of Different Methods over AR Database with 2580D (Coding over [D E]).

Corruptions	White Gaussian Noise					Random Pixel Corruption				
	10%	30%	50%	70%	90%	10%	30%	50%	70%	90%
CESR [13]	91.85%	87.15%	82.08%	71.85%	57.62%	91.38%	91.15%	90.23%	76.85%	8.08%
LRC [17, 19]	93.00%	92.46%	91.69%	90.15%	87.15%	92.15%	84.92%	51.15%	8.54%	1.77%
CRC-RLS [18]	93.00%	92.46%	91.69%	89.23%	87.15%	92.15%	84.92%	51.15%	8.54%	1.77%
LCCR + Cityblock	93.39%	93.00%	92.15%	90.15%	87.39%	93.08%	88.23%	70.15%	34.08%	5.08%
LCCR + Seucclidean	93.31%	93.00%	92.15%	90.15%	87.31%	92.69%	85.85%	51.39%	8.62%	2.46%
LCCR + Euclidean	93.31%	92.77%	91.92%	90.31%	87.62%	92.62%	86.00%	52.46%	10.69%	2.54%
LCCR + Cosine	93.15%	93.23%	92.23%	90.39%	87.77%	92.69%	85.62%	51.59%	8.62%	2.77%
LCCR + Spearman	93.39%	93.15%	92.62%	90.54%	88.31%	93.31%	88.54%	77.00%	56.54%	13.62%

- 389 [8] E. Elhamifar, R. Vidal, Sparse subspace clustering: Algorithm, theory, and applications, To appear in IEEE Transactions on Pattern Analysis
390 and Machine Intelligence.
- 391 [9] C. Wang, X. He, J. Bu, Z. Chen, C. Chen, Z. Guan, Image representation using laplacian regularized nonnegative tensor factorization, Pattern
392 Recognition 44 (10) (2011) 2516–2526.
- 393 [10] J. Wright, A. Y. Yang, A. Ganesh, S. S. Sastry, Y. Ma, Robust face recognition via sparse representation, IEEE Transactions on Pattern
394 Analysis and Machine Intelligence 31 (2) (2009) 210–227.
- 395 [11] H. Zhang, N. M. Nasrabadi, Y. Zhang, T. S. Huang, Joint dynamic sparse representation for multi-view face recognition, Pattern Recognition
396 45 (4) (2012) 1290–1298. doi:10.1016/j.patcog.2011.09.009.
- 397 [12] H. Zhang, Y. Zhang, T. S. Huang, Simultaneous discriminative projection and dictionary learning for sparse representation based classifica-
398 tion, Pattern Recognition 46 (1) (2013) 346–354.
- 399 [13] R. He, W.-S. Zheng, B.-G. Hu, Maximum correntropy criterion for robust face recognition, IEEE Transactions on Pattern Analysis and
400 Machine Intelligence 33 (8) (2011) 1561–1576.
- 401 [14] S. Z. Li, J. Lu, Face recognition using the nearest feature line method, IEEE Transactions on Neural Networks 10 (2) (1999) 439–443.
- 402 [15] J. Yang, L. Zhang, Y. Xu, J. Yang, Beyond sparsity: The role of l1-optimizer in pattern classification, Pattern Recognition 45 (3) (2012)
403 1104–1118.
- 404 [16] R. Rigamonti, M. A. Brown, V. Lepetit, Are sparse representations really relevant for image classification?, in: Proc. of IEEE International
405 Conference on Computer Vision and Pattern Recognition, 2011, pp. 1545–1552.
- 406 [17] Q. Shi, A. Eriksson, A. van den Hengel, C. Shen, Is face recognition really a compressive sensing problem?, in: Proc. of IEEE Conference
407 on Computer Vision and Pattern Recognition.
- 408 [18] L. Zhang, M. Yang, X. Feng, Sparse representation or collaborative representation: Which helps face recognition?, in: Proc. of IEEE
409 International Conference on Computer Vision.
- 410 [19] I. Naseem, R. Togneri, M. Bennamoun, Linear regression for face recognition, IEEE Transactions on Pattern Analysis and Machine Intelli-
411 gence 32 (11) (2010) 2106–2112.
- 412 [20] X. He, D. Cai, S. Yan, H. Zhang, Neighborhood preserving embedding, in: Proc. of IEEE International Conference on Computer Vision.
- 413 [21] M. Belkin, P. Niyogi, V. Sindhwani, Manifold regularization: A geometric framework for learning from labeled and unlabeled examples, The
414 Journal of Machine Learning Research 7 (2006) 2399–2434.
- 415 [22] S. C. Yan, D. Xu, B. Y. Zhang, H. J. Zhang, Q. Yang, S. Lin, Graph embedding and extensions: A general framework for dimensionality
416 reduction, IEEE Transactions on Pattern Analysis and Machine Intelligence 29 (1) (2007) 40–51.
- 417 [23] R. G. Baraniuk, M. B. Wakin, Random projections of smooth manifolds, Foundations of Computational mathematics 9 (1) (2009) 51–77.
- 418 [24] A. Majumdar, R. K. Ward, Robust classifiers for data reduced via random projections, IEEE Transactions on Systems, Man, and Cybernetics,
419 Part B: Cybernetics 40 (5) (2010) 1359–1371. doi:10.1109/TSMCB.2009.2038493.
- 420 [25] J. Wang, J. Yang, K. Yu, F. Lv, T. Huang, Y. Gong, Locality-constrained linear coding for image classification, in: Proc. of IEEE International
421 Conference on Computer Vision and Pattern Recognition, 2010, pp. 3360–3367.
- 422 [26] S. T. Roweis, L. K. Saul, Nonlinear dimensionality reduction by locally linear embedding, Science 290 (5500) (2000) 2323–2326.
- 423 [27] Y. Chao, Y. Yeh, Y. Chen, Y. Lee, Y. Wang, Locality-constrained group sparse representation for robust face recognition, in: Proc. of IEEE
424 International Conference on Image Processing, 2011, pp. 761–764.
- 425 [28] M. Yang, L. Zhang, D. Zhang, S. Wang, Relaxed collaborative representation for pattern classification, in: Proc. of IEEE Conference on
426 Computer Vision and Pattern Recognition, 2012, pp. 2224–2231.
- 427 [29] K. Ohki, S. Chung, Y. H. Ch'ng, P. Kara, R. C. Reid, Functional imaging with cellular resolution reveals precise micro-architecture in visual
428 cortex, Nature 433 (7026) (2005) 597–603.
- 429 [30] X. He, S. Yan, Y. Hu, P. Niyogi, H. Zhang, Face recognition using laplacianfaces, IEEE Transactions on Pattern Analysis and Machine
430 Intelligence 27 (3) (2005) 328–340.
- 431 [31] M. R. Osborne, B. Presnell, B. A. Turlach, A new approach to variable selection in least squares problems, IMA Journal of Numerical
432 Analysis 20 (3) (2000) 389–403.
- 433 [32] X. Peng, L. Zhang, Z. Yi, Scalable sparse subspace clustering, in: Proc. of IEEE Conference on Computer Vision and Pattern Recognition,
434 2013.
- 435 [33] A. Martinez, R. Benavente, The ar face database (1998).
- 436 [34] F. Samaria, A. Harter, Parameterisation of a stochastic model for human face identification, in: Proc. of the IEEE Workshop on Applications
437 of Computer Vision (WACV), 1994, pp. 138–142.
- 438 [35] A. Georghiades, P. Belhumeur, D. Kriegman, From few to many: illumination cone models for face recognition under variable lighting and
439 pose, IEEE Transactions on Pattern Analysis and Machine Intelligence 23 (6) (2001) 643–660.
- 440 [36] R. Gross, I. Matthews, J. Cohn, T. Kanade, S. Baker, Multi-pie, Image and Vision Computing 28 (5) (2010) 807–813.

- 441 [37] R.-E. Fan, K.-W. Chang, C.-J. Hsieh, X.-R. Wang, C.-J. Lin, Liblinear: A library for large linear classification, *Journal of Machine Learning*
442 *Research* 9 (2008) 1871–1874.
- 443 [38] M. Turk, A. Pentland, Eigenfaces for recognition, *Journal of Cognitive Neuroscience* 3 (1) (1991) 71–86.
- 444 [39] M. Grant, S. Boyd, Graph implementations for nonsmooth convex programs, in: V. Blondel, S. Boyd, H. Kimura (Eds.), *Recent Advances in*
445 *Learning and Control, Lecture Notes in Control and Information Sciences*, Springer-Verlag Limited, 2008, pp. 95–110.
- 446 [40] M. Savvides, R. Abiantun, J. Heo, S. Park, C. Xie, B. Vijayakumar, Partial holistic face recognition on frgc-ii data using support vector
447 machine, in: *Proc. of Computer Vision and Pattern Recognition Workshop*, 2006, pp. 48–53.
- 448 [41] P. Sinha, B. Balas, Y. Ostrovsky, R. Russell, Face recognition by humans: Nineteen results all computer vision researchers should know
449 about, *Proceedings of the IEEE* 94 (11) (2006) 1948–1962.
- 450 [42] L. S. Qiao, S. C. Chen, X. Y. Tan, Sparsity preserving projections with applications to face recognition, *Pattern Recognition* 43 (1) (2010)
451 331–341.